Meccanica **36:** 131–150, 2001.

Multiresolution Analysis of Elastic Degradation in Heterogeneous Materials

KASPAR WILLAM, INKYU RHEE and GREGORY BEYLKIN
University of Colorado at Boulder, Department of Civil Engineering; Boulder CO 80309-0428, U.S.A.

(Accepted: 12 June 2001)

Abstract. In this study we examine the stiffness properties of heterogeneous elastic materials and their degradation at different levels of observations. To this end we explore the opportunities and limitations of multiresolution wavelet analysis, where successive Haar transformations lead to a recursive separation of the stiffness properties and the response into coarse- and fine-scale features. In the limit, this recursive process results in which are immersed in a hardened cement paste taking due account of the mismatch of the two elastic constituents.

Sommario. In questo studio si esaminano le proprietà di rigidezza di materiali elastici eterogenei ed il loro degrado a diverse scale di osservazione. A questo scopo si esplorano le opportunità e le limitazioni di analisi con *wavelets* a risoluzione multipla, dove successive trasformazioni di Haar conducono ad una separazione ricorsiva delle proprietà della rigidezza e della risposta nelle loro caratteristiche di scala fine e grossolana. Al limite, questo processo ricorsivo dà luogo ad un parametro di omogeneizzazione che rappresenta una misura media della rigidezza e della capacità di immagazzinare energia di deformazione alla grande scala. Il concetto di base dell'analisi a risoluzione multipla è illustrato per mezzo di problemi modello mono- e bi-dimensionali che si riferiscono ad un composito particolato a due fasi rappresentativo della morfologia del calcestruzzo. Le caratteristiche microstrutturali del calcestruzzo sono modellate nello studio computazionale sotto forma di un sistema a due materiali di particelle aggregate, immerse in una pasta di cemento indurita e tenendo conto della mancata congruenza tra i due costituenti elastici.

Key words: Multiresolution homogenization, Haar wavelets42.5ts42.5t2eagwcni22anianiani69chen-33*u3 anidaremtio*u3 enaeme1. Introd

Traditionally, engineering materials are considered to be macroscopically homogeneous and often isotropic. While in most applications this approach may be adequate, progressive degradation processes can only be explained properly by considering micro-structural events which take place at the fine scales of materials. This requires characterization of each constituent and their interface conditions, in addition to the morphology of the specific meso- and micro-structures, respectively. This type of study is very demanding in terms of manpower and computing resources, in spite of the recent computational advances in model-based simulations in three-dimensional space and time.

(a) *Multi-Physics Interaction*: Deterioration of materials is induced by the mismatch of the constituents in heterogeneous materials and environmental factors, which include temper-

2. Partitioning

Aside from the challenge of modeling progressive damage, there are several significant mathematical issues which are central to the entire field of deterioration analysis. One of them deals with upscaling the fine resolution of heterogeneities to the coarse system of homogenized materials. The other deals with the loss of positive material properties when damage and degradation takes place at the fine level of observation and its manifestation at the coarse level of homogenization.

2.1. Two-Scale Scale Analysis

The mathematical background of deterioration analysis centers around two concepts, (i) partitioning of the algebraic/differential system which turns increasingly ill-conditioned as the elastic stiffness properties deteriorate, and (ii) measuring deterioration in space and time in terms of effective damage measures at different scales.

Partitioning dates back to early work of Schur (1917) who among many important contributions to matrix analysis decomposed the solution domain into non-overlapping subdomains. In the elementary example of a linear algebraic problem the unknown solution vector $\boldsymbol{r}$ is decomposed into two groups of unknowns $\boldsymbol{r}_1, \boldsymbol{r}_2$, which describe the coarse and fine scale response in the case of wavelet transformations discussed later on.

$$\begin{bmatrix} \boldsymbol{K}_{11} & \boldsymbol{K}_{12} \\ \boldsymbol{K}_{21} & \boldsymbol{K}_{22} \end{bmatrix} \begin{bmatrix} \boldsymbol{r}_1 \\ \boldsymbol{r}_2 \end{bmatrix} = \begin{bmatrix} \boldsymbol{f}_1 \\ \boldsymbol{f}_2 \end{bmatrix} . \tag{1}$$

In the case of environmental and mechanical deterioration, the solution domain decomposes naturally into:730.itespoTj0.022 -0.3.30010 0 7.5716 2Tc(22)Tj19 Tm0.0071 Tc(22)Tj/F5 1 Tf10.9091 0 0 10.909

a '*size-effect*' which transports localized defects from the micro-scale of observation to the macro-scale of homogenized continua which differs, however, from the fracture

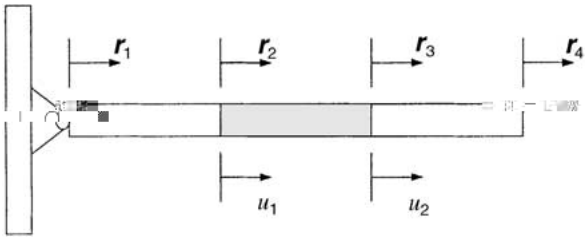

Figure 1. Deterioration due to element erosion in one-dimensional bar structure, $EA/L = 1$.

of the intermediate element are deteriorating progressively according to the traditional format of scalar damage

$$\sigma = E_s \epsilon \quad \text{where} \quad E_s = [1 - D_E]E_o \quad \text{with} \quad D_E = 1 - \frac{E_s}{E_o}. \tag{6}$$

Here E_o denotes the initial intact elastic modulus of elasticity, and D_E indicates the level of damage as a measure of the secant to the initial stiffness ratio. Considering different values of damage, $0 \leqslant D_E \leqslant 1$, Figure 2 illustrates the effect of material deterioration in the intermediate element on the spectral properties of the structure. In the present case of scalar damage, the element secant stiffness deteriorates proportionally to the material damage, that is

$$\boldsymbol{k}_s = \frac{[\Delta - D_E]E_o A}{L} \begin{bmatrix} 1 & -1 \\ -1 & 1 \end{bmatrix}, \tag{7}$$

where $E_o A/L = 1$. Though the non-zero element eigenvalue decreases proportionally with progressive material damage, $\lambda_k = [1 - D_E]E_o A/L$, we observe in Figure 2(a) that deterioration at the structural level leads to non-proportional deterioration of all three eigenvalues. Normalization or rather pre-conditioning with the intact flexibility matrix $\boldsymbol{K}_o^{-1}$ separates the damage according to the rank-one update argument above, and leads to the spectral properties shown in Figure 2(b). We recognize, that pre-conditioning isolates the damage into a single

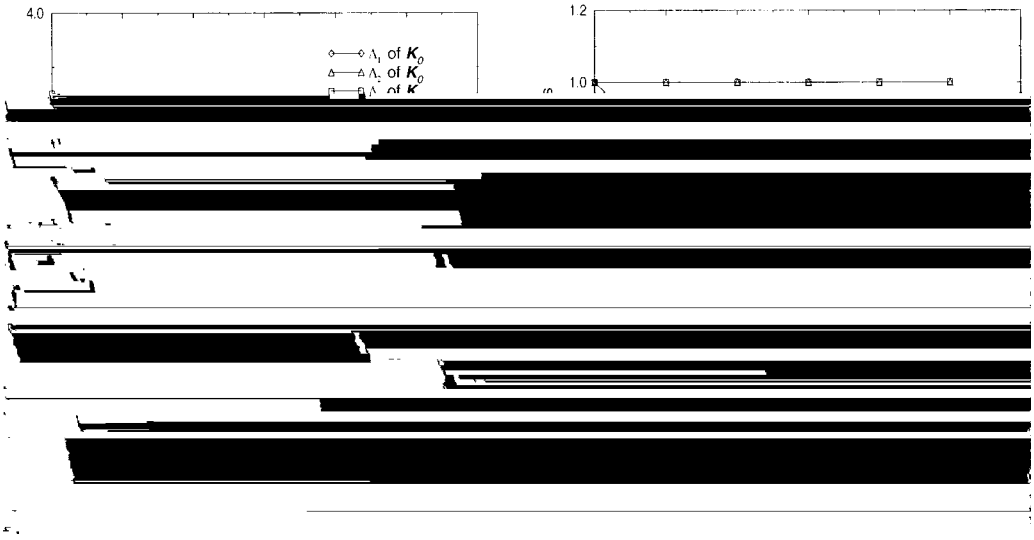

Figure 2. Three bar problem: variation of (a) eigenvalues, (b) normalized eigenvalues of structural assembly.

(c) they introduce compact representation: the coefficients of a wavelet transfomation will

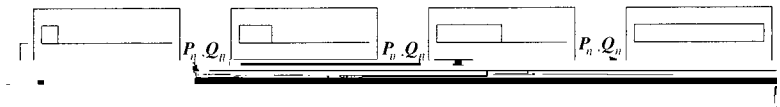

Figure 6. The Haar wavelet basis.

Figure 6 illustrates the sequence of scaling and wavelet transformations of three reductions by summing and differencing the unit step functions.

As previously mentioned, Φ_j is the basis for V^j. Applying Equations 10 and 11 with $j = 3$ to the functions $\phi_{3k}(t) = \phi(2^3 t - k),\ k = 0, \cdots, 7$ yields the functions $\phi_{2k}(t) = \phi(2^2 t - k),\ k = 0, \cdots, 3$ and $\psi_{2k}(t) = \psi(2^2 t - k),\ k = 0, \cdots, 3$.

In general, the Haar wavelet basis of V^j contains 2^j functions.

4. Multiresolution Homogenization

There are many important physical problems which incorporate several scales of observation. In heterogeneous media we typically encounter fine (microscopic) scale and coarse (macroscopic) scale features. Typically, '*homogenization*' methods require that the fine scale behavior is fairly well separated from the behavior on the coarse scales. Recently, a multiresolution analysis (MRA) has been proposed by Beylkin and Coult (1998) for homogenizing the transition between adjacent scales. This recursive procedure involves sequential steps of reduction as opposed to reconstruction, which may be repeated over many scales.

The basic step of the reduction involves computing a Schur complement which plays an important role in algebraic multigrid and domain decomposition methods. Thereby, the form of equations is fully preserved so that one can use the reduction step in a recursive manner.

The main idea of the MRA scheme is illustrated best with the linear algebraic example

$$\boldsymbol{K}\,\boldsymbol{r} = \boldsymbol{f}, \tag{20}$$

where $\boldsymbol{K}$ is a matrix of size $2^n \times 2^n$. We change basis by an orthogonal transformation with the discrete Haar transform by writing,

$$\boldsymbol{r}_s = \frac{1}{\sqrt{2}}(\boldsymbol{r}_{2k+1} + \boldsymbol{r}_{2k}) \quad \text{and} \quad \boldsymbol{r}_d = \frac{1}{\sqrt{2}}(\boldsymbol{r}_{2k+1} - \boldsymbol{r}_{2k}) \tag{21}$$

for $k = 0, \cdots, 2^{n-1} - 1$. The elements of $\boldsymbol{r}_s$ are essentially averages of neighboring entries in $\boldsymbol{r}$ (they have an extra factor $\sqrt{2}$ when compared with true averages) and the elements

of $\boldsymbol{r}_d$ are differences. We can write the discrete Haar transform as a matrix $\boldsymbol{M}_n$ of size $2^n \times 2^n$:

$$\boldsymbol{M}_n = \frac{1}{\sqrt{2}} \begin{bmatrix} 1 & 1 & 0 & 0 & & & \cdots \\ 0 & 0 & 1 & 1 & 0 & 0 & \cdots \\ & & & \ddots & & & \\ -1 & 1 & 0 & 0 & & & \cdots \\ 0 & 0 & -1 & 1 & 0 & 0 & \cdots \\ & & & \ddots & & & \end{bmatrix}. \tag{22}$$

If we denote the top half of $\boldsymbol{M}_n$ by $\boldsymbol{P}_n$ and the bottom half by $\boldsymbol{Q}_n$, then

$$\boldsymbol{M}_n^t \boldsymbol{M}_n = \boldsymbol{M}_n \boldsymbol{M}_n^t = \boldsymbol{Q}_n^t \boldsymbol{Q}_n + \boldsymbol{P}_n^t \boldsymbol{P}_n = \boldsymbol{I} \quad \text{and} \quad \boldsymbol{Q}_n \boldsymbol{Q}_n^t = \boldsymbol{I} = \boldsymbol{P}_n \boldsymbol{P}_n^t. \tag{23}$$

Splitting the linear system in Equation 20 into two sets of equations in the two unknowns, $\boldsymbol{P}_n \boldsymbol{r} = \boldsymbol{r}_s$ and $\boldsymbol{Q}_n \boldsymbol{r} = \boldsymbol{r}_d$, and applying $\boldsymbol{P}_n$ to both sides, we get after dropping subscripts,

$$\boldsymbol{P}\boldsymbol{K}\boldsymbol{r} = (\boldsymbol{P}\boldsymbol{K}\boldsymbol{P}^t)\boldsymbol{P}\boldsymbol{r} + (\boldsymbol{P}\boldsymbol{K}\boldsymbol{Q}^t)\boldsymbol{Q}\boldsymbol{r} = \boldsymbol{P}\boldsymbol{f}. \tag{24}$$

where

$$\begin{aligned} \boldsymbol{K}_{ss} &= \boldsymbol{P}_{n-j}\boldsymbol{K}_j\boldsymbol{P}^t_{n-j}, \quad \boldsymbol{K}_{sd} = \boldsymbol{P}_{n-j}\boldsymbol{K}_j\boldsymbol{Q}^t_{n-j}, \\ \boldsymbol{K}_{ds} &= \boldsymbol{Q}_{n-j}\boldsymbol{K}_j\boldsymbol{P}^t_{n-j}, \quad \boldsymbol{K}_{dd} = \boldsymbol{Q}_{n-j}\boldsymbol{K}_j\boldsymbol{Q}^t_{n-j}. \end{aligned} \tag{31}$$

This recursion process involves only the matrices $\boldsymbol{K}_j$ and the vector $\boldsymbol{f}_j$. In other words, we do not have to solve for $\boldsymbol{r}$ at any step in the reduction procedure. If we apply this reduction process n times, we obtain a '*scalar*' SDOF equation which can be readily solved for $s$olv698-253. 729.2yad2.

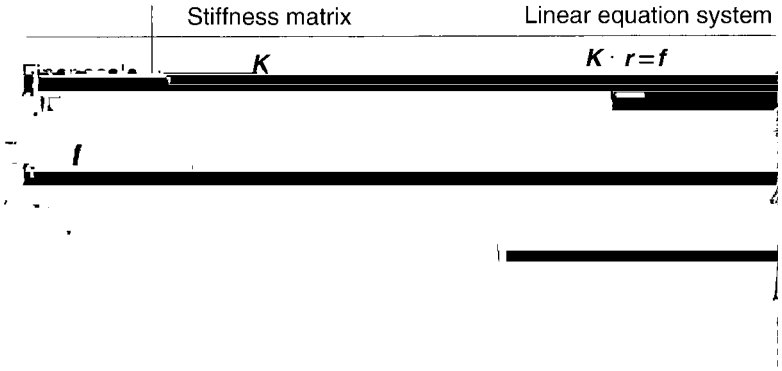

Figure 7. MRA reduction procedure.

The ellipticity estimate of Equation 35 raises the important question under which conditions do the lower eigenvalues of $\boldsymbol{K}_j$ coincide with the eigenvalues of $\boldsymbol{R}_j$ and how close are the upper bounds. Clearly, the answer to this question depends on how well the fundamental modes of the unreduced system are captured by the reduced system.

6. Homogenization of Two-phase Particle Composites

In what follows we consider the homogenization of a two-phase particle composite which is made up of elastic aggregate inclusions which are embedded in an elastic matrix. For illustration we compare homogenization via MRA in one- and two-dimensions in order to assess the validity of the homogenization parameter and its bounding property when compared to averaging the numerical FEM results.

6.1. One-dimensional Model Problem

To start with we consider a periodic arrangement of stiff particles and weak matrix constituents in the one-dimensional simulation model shown in Figure 8, for which analytical solutions are readily available from homogenization.

Assuming linear elastic behavior of the two materials with a contrast ratio of the stiffness properties $E_a/E_m = 3$ with $E_m = 10$, the spectral properties of the $n$dof $= 2^6 = 64$ simulation with 64 bar elements of size $h = 1$ range from $\lambda_{\min} = 8.82701 \times 10^{-3}$ to

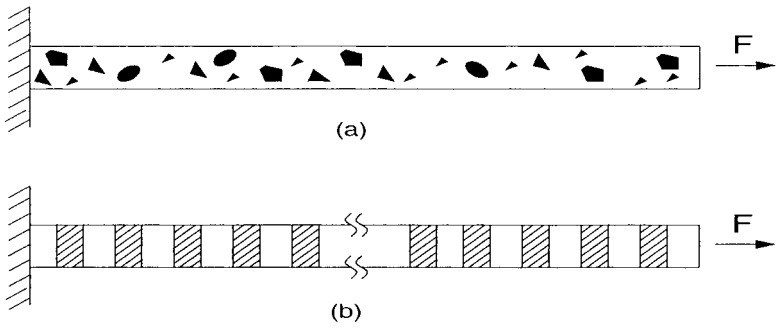

Figure 8. One-dimensional axial bar problem made of periodic two-phase material.

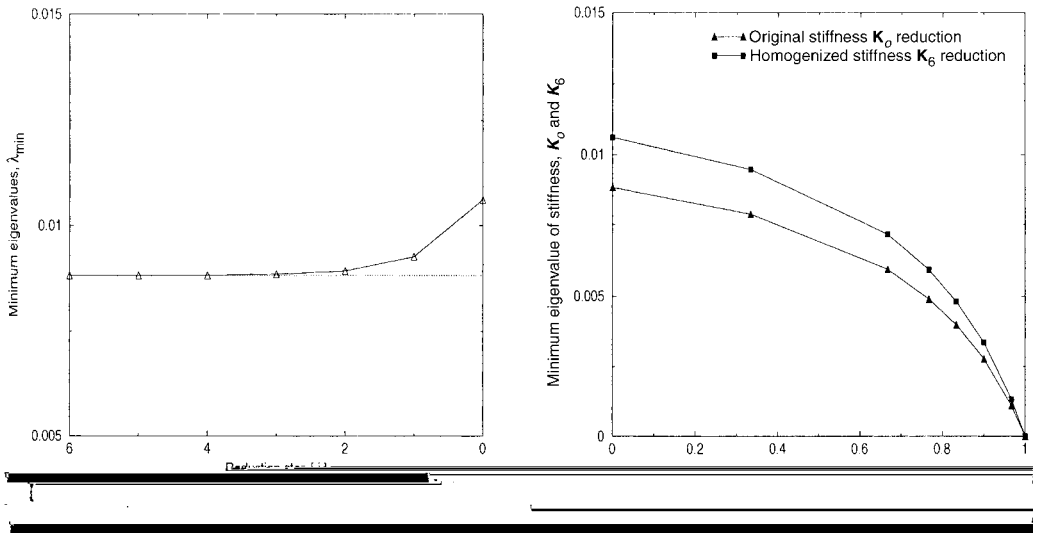

Figure 9. One-dimensional axial bar problem: (a) upper bound properties of minimum eigenvalues at different cycles of reduction in one-dimensional, (b) variation of minimum eigenvalue of stiffness, $\boldsymbol{K}_o$ and $\boldsymbol{K}_6$ due to progressive deterioration of aggregate stiffness.

$\lambda_{\max} = 7.$

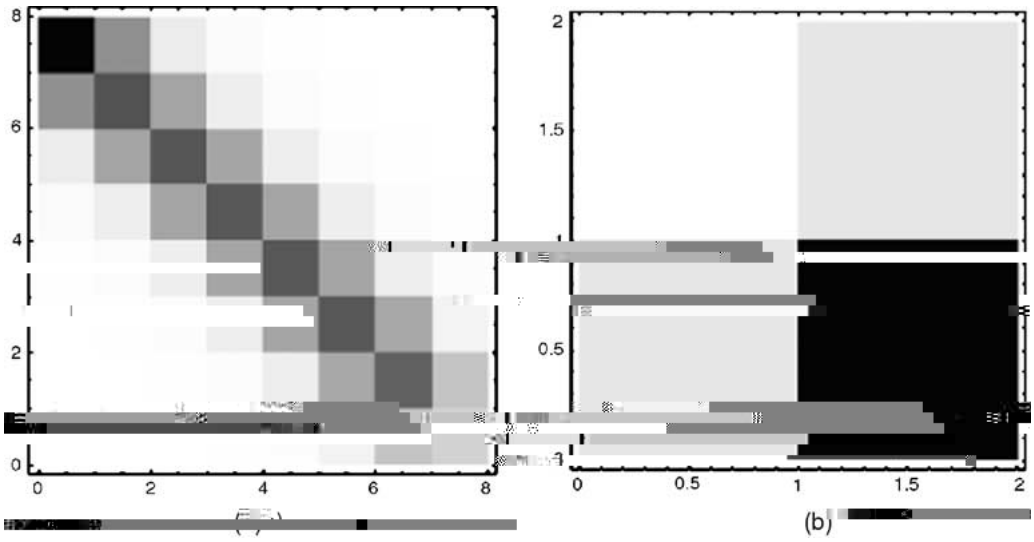

Figure 12. One-dimensional axial bar problem, density plot of stiffness matrix: (a) $\boldsymbol{K}_3 \in \mathcal{R}^8$, (b) $\boldsymbol{M}_1 \boldsymbol{K}_1 \boldsymbol{M}_1^t \in \mathcal{R}^1$.

In short, MRA provides a homogenized stiffness property which reproduces exactly the average response for a given load scenario, whereby the resulting homogenization parameter maintains a close upper bound of the lowest eigenvalue of the unreduced bar structure.

6.2. Two-dimensional Model Problem

In what follows we consider homogenization of the two-phase particle composite in two-dimension as indicated in Figures 13(a) and (b).

Assuming isotropic linear elastic behavior of the two materials with a contrast ratio of the stiffness properties $E_a/E_m = 3$ and $\nu_a/\nu_m = 0.5$, the spectral properties of the $n$dof =

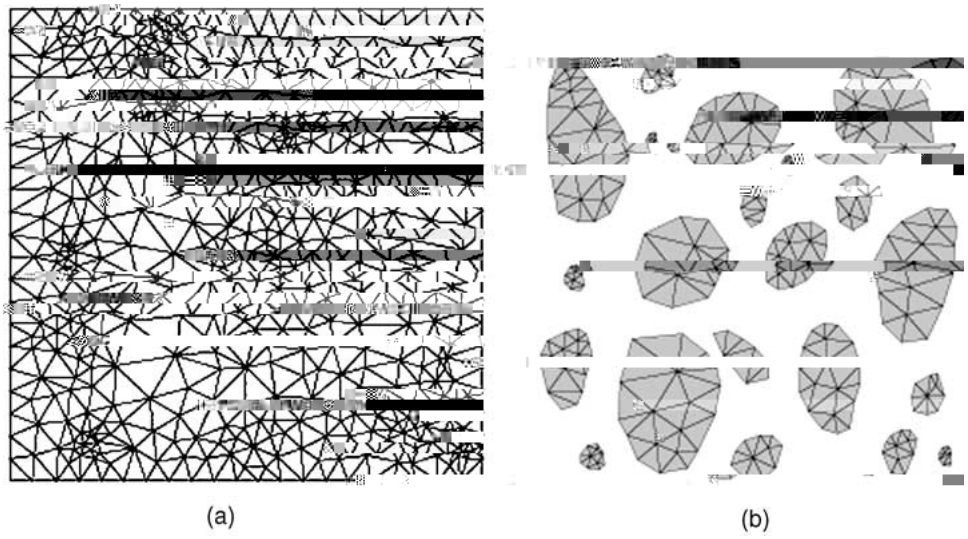

Figure 13. Two-dimensional composite structure: (a) overall mesh (b) aggregates mesh.

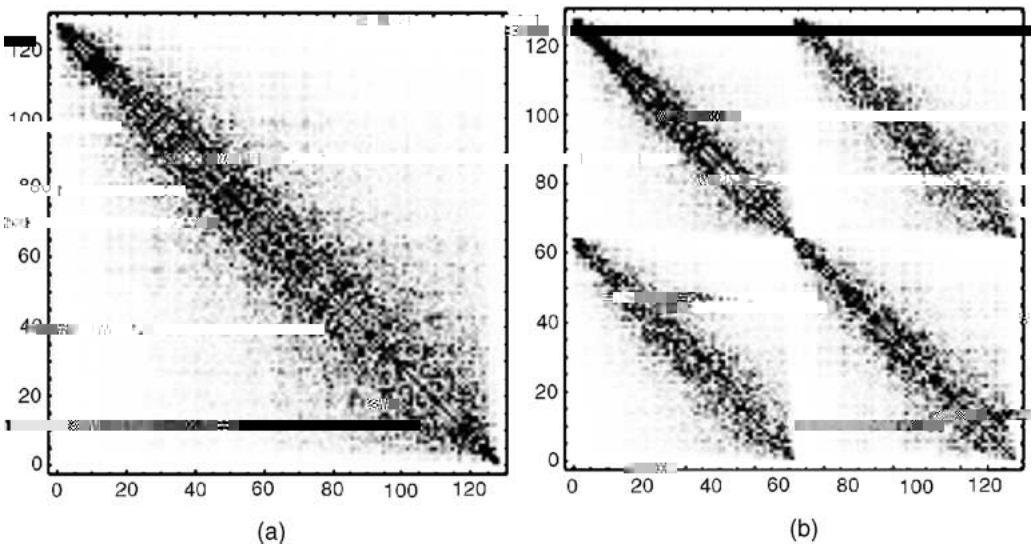

Figure 14. Two-dimensional composite structure, density plot of stiffness matrix: (a) $\boldsymbol{K}_7 \in \mathcal{R}^{128}$, (b) $\boldsymbol{M}_7\boldsymbol{K}_7\boldsymbol{M}_7^t \in \mathcal{R}^{128}$.

$2^{10} = 1024$ simulation range from $\lambda_{\min} = 5.293 \times 10^{-2}$ to $\lambda_{\max} = 2.125 \times 10^{2}$. Given the volume fraction of the aggregate particles, $V_a = 0.346917$, the Hashin–Shtrikman bounds of

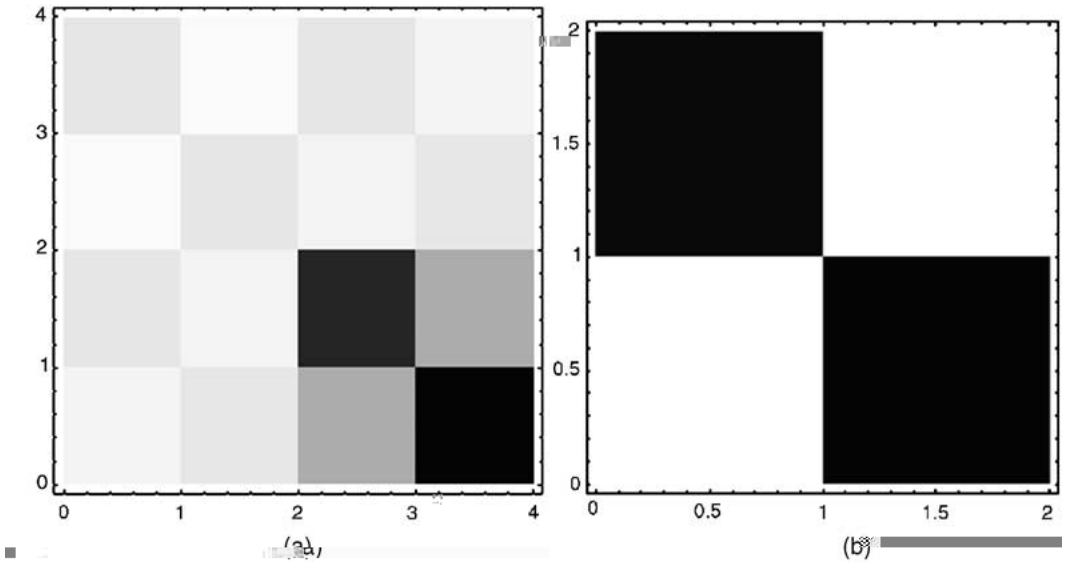

Figure 16. Two-dimensional composite structure, density plot of separating x-, y-stiffness coefficients: (a) $\boldsymbol{M}_2 \boldsymbol{K}_2 \boldsymbol{M}_2^t \in \mathcal{R}^4$, (b) $\boldsymbol{M}_1 \boldsymbol{K}_1 \boldsymbol{M}_1^t \in \mathcal{R}^2$.

the absolute magnitude of the stiffness coefficients in the coarse and fine partitions at different levels of observation.

6. Gilbert, A., ‘A comparison of multiresolution and classical homogenization schemes’, *Appl. Comput. Harmonic Anal.* **5** (1998) 1–35.
7. Haar, A., ‘Zur theorie der orthogonalen funktionensysteme’, *Math. Annalen* **69** (1910) 331–371.
8. Hashin, Z., ‘Analysis of composite materials’, *J. Appl. Mech., ASME* **50** (1987) 481–505.
9. Rizzi, E., Maier, G. and Willam, K., ‘On failure indicators in multi-dissipative materials’, *Int. J. Solids Struct.* **33**(20–22) (1996) 3187–3214.
10. Schur, I., ‘*Ein Beitrag zur Additiven Zahlentheorie und zur Theorie der Kettenbrüche’*, S.B. Preuss. Akad. Wiss. Phys-Math. Kl. 1917, pp. 302–321 (reprinted in: I. Schur, Gesammelte Abhandlungen, Vol. 2, Springer Verlag, 1973, pp. 117–136).
11. Steinberg, B.Z. and McCoy, J.J., ‘A class of one-dimensional stiffness microstructures resulting in identical macroscale response’, *Wave Motion* **23** (1996) 237–258.
12. Willam, K. and Rhee, I., ‘Deterioration analysis of materials and structures’, *Engng Comput.* (2000) (in press).